Controlled formation and size-selected deposition of indium nanoparticles from a microwave flow reactor on semiconductor surfaces

Klemens Hitzbleck, Hartmut Wiggers, and Paul Roth

Citation: Applied Physics Letters **87**, 093105 (2005); doi: 10.1063/1.2012516
View online: http://dx.doi.org/10.1063/1.2012516
View Table of Contents: http://scitation.aip.org/content/aip/journal/apl/87/9?ver=pdfcov
Published by the AIP Publishing

Controlled formation and size-selected deposition of indium nanoparticles from a microwave flow reactor on semiconductor surfaces

Klemens Hitzbleck, Hartmut Wiggers, and Paul Roth[a)]
Institut für Verbrennung und Gasdynamik, Universität Duisburg-Essen, 47057 Duisburg, Germany

(Received 22 February 2005; accepted 28 June 2005; published online 22 August 2005)

Indium nanoparticles were synthesized in a microwave flow reactor by thermal decomposition of trimethylindium. The particles were extracted from the gas phase by molecular beam sampling, deflected in an electric field, and deposited on a semiconductor surface. The size of the deposited particles was selected by adjusting the deflection voltage. The geometric standard deviation of the size-selected particles was found to be smaller than 10%. The deposition method is compatible with epitaxial growth methods and enhances their potentials with nanoparticle technology. © *2005 American Institute of Physics*. [DOI: 10.1063/1.2012516]

Nanosized materials have properties that differ from the corresponding bulk behavior, making them attractive for new applications in materials science[1–3] and nano electronics.[4–7] As a result of the nanoscaled dimensions, quantum effects are becoming important, opening new applications, particularly with regard to semiconductor technology, e.g., quantum dots in semiconductor structures. An established method to generate such structures is the self-organized growth of quantum dots by the Stranski–Krastanov mode.[8] This method is based on epitaxial distension and works for certain material combinations determined by atomic structure and size. It has been successfully applied for a lot of quantum dot devices, for instance quantum dot lasers.[9] Nevertheless, the Stranski–Krastanov growth is limited in terms of material, size, and deposition density of quantum dots. A possibility to overcome these restrictions is the deposition (and subsequent embedding) of pre-produced nanoparticles within a semiconductor structure. To this purpose, several deposition methods are possible,[10] but with respect to purity and surface composition, particles from gas phase synthesis are preferred compared to materials from wet synthesis with surface active additives.[11]

A lot of groups deal with size separation by means of low pressure operating differential mobility analysis (DMA).[12,13] This system has been successfully applied for high deposition rates at an operating pressure of a few mbar. Nevertheless, DMA technology is not compatible in pressure with metal organic vapor phase epitaxy (MOVPE) and metal organic chemical vapor deposition (MOCVD), since an additional pressure stage is necessary while the deposition rate drops. There are a couple of methods available, consisting of low pressure particle formation combined with high vacuum extraction.[11] Several of these methods have been applied for size selected deposition, but usually these methods suffer from the disadvantage that they produce comparatively low particle concentration. This paper focuses on a method that is compatible in pressure and purity with epitaxial conditions and enables high deposition rates of up to 10^7 size-selected particles/s with very narrow size distribution. Details of the experimental setup have been reported elsewhere,[14,15] but it is composed of a low pressure microwave plasma reactor for the synthesis of charged nanoparticles and a particle mass spectrometer (PMS) described by Hospital and Roth for the particle deposition.[16]

The solid precursor TMIn was vaporized and mixed with argon in an online mixing device similar to well-established techniques used for MOVPE. The precursor concentration was varied between 200 and 500 ppm. A molecular beam sampling system, located downstream the plasma zone, was used to extract particles from the reactive zone for PMS analysis and surface deposition. A glass nozzle helps to form a free-jet by directing a sample from the low pressure particle formation region into a vacuum chamber ($p = 10^{-3}$ mbar). The supersonic expansion into the free-molecular regime leads to a rapid decrease in temperature, which suppresses further chemical and physical processes almost completely. The center of the free-jet is then extracted by a skimmer and propagates as a particle loaded molecular beam into the analysis chamber ($p = 10^{-6}$ mbar), where PMS analysis and particle deposition is performed.

The principle of the PMS is based on the behavior of charged particles in an electric field. The particle loaded molecular beam is directed through a deflection capacitor which separates charged particles according to their mass, velocity, and charge. Particles from the deflected molecular beam can pass an aperture and are detected, if their properties fulfill the following condition:

$$Kmv^2 = n_e e U_D, \tag{1}$$

where K is a geometric constant, n_e the number of elementary charges e per particle, U_D the deflection voltage, m the particle mass, and v the particle velocity. Figure 1 shows a schematic drawing of the analysis chamber. Our laboratory-made system consists of a deflection capacitor (copper, 70 mm long, separation distance 20 mm), and a 5 mm aperture 300 mm downstream. The particles passing the aperture slit can either be counted by a Faraday cup or are sampled on a surface. TEM grids and substrates can be positioned by means of an adjustable holder in the particle beam. A mechanical shutter allows a time-controlled deposition of particles on a substrate.

The geometry of the PMS is optimized to measure particles in the size range of 2 to 15 nm. According to Fuchs' equation,[17] the probability to synthesize single charged particle is 32% in case of particles with a diameter of 15 nm,

[a)]Author to whom correspondence should be addressed; electronic mail: roth@ivg.uni-duisburg.de

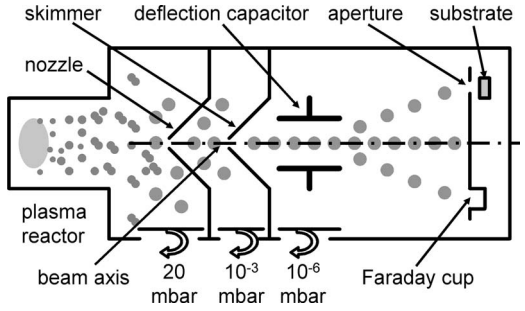

FIG. 1. Schematic setup for nanoparticle synthesis and analysis chamber with the PMS. The particles are deposited through the aperture on a substrate.

which drops to 1% for double charged particles. With reduced size, the probability of multiple charges tends almost to zero. A typical beam current for size-selected particles is a few picoamperes, equivalent to $\sim 10^7$ particles/s. They are deposited through an aperture of 5 mm in diam placed in front of the Faraday cup and the sample, respectively.

The velocity of the particles is measured by use of two repelling potentials operated with a frequency tunable square wave signal between 10 and 10^4 Hz. With decreasing frequency, an oscillating current is observed at the Faraday cup, whereby the relation between the particle velocity v and the frequency difference between two minima of the measured current (Δf) is

$$v = \Delta f l_g, \tag{2}$$

where l_g is the distance between the potential grids. With known velocity and charge, the mass of the particles can be determined according to Eq. (1), see also Ref. 16.

Indium nanoparticles with a specific size were synthesized by the decomposition of TMIn in the microwave plasma reactor and their mass was investigated by means of the PMS. Figure 2 shows a typical probability density function determined from PMS measurements. The calculated count median diameter of the particles (CMD) is 5.8 nm with a geometric standard deviation of $\sigma_g = 1.2$.

A certain fraction of this particle ensemble was selected by adjusting the deflection voltage to 10 V corresponding to a particle size of 6 nm (see dotted line in Fig. 2). The size-selected particles were deposited on TEM grids as well as on substrates, see Fig. 3. The sampled particles show spherical morphology and monodispersity, and no agglomeration. Micrographs of different areas on the TEM grid were analyzed

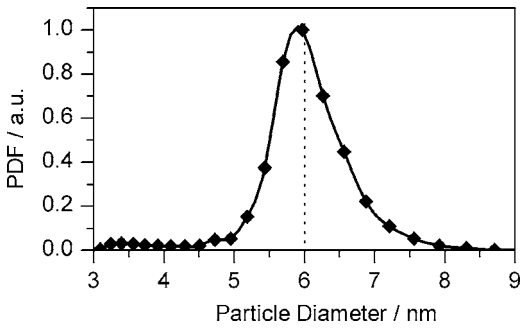

FIG. 2. Probability density function of the synthesized particles measured by PMS. Due to the chosen experimental conditions, particles with a CMD of 5.8 nm and a geometric standard variation of $\sigma_g = 1.2$ are produced. The dotted line marks the particles section selected for deposition.

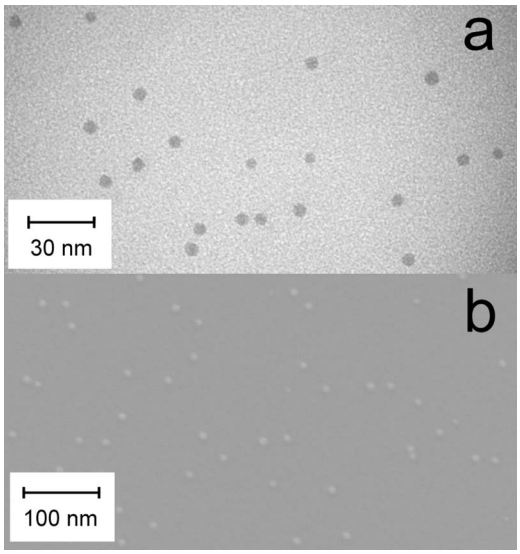

FIG. 3. (a) TEM micrograph of Indium particles with a selected diameter of 6 nm deposited on a TEM-grid for image analysis, (b) SEM image of a silicon substrate after deposition of size selected indium particles.

to obtain the size distribution of the deposited particles. Figure 4 summarizes the result of the image analysis. The size parameters calculated from a lognormal fit were CMD $= 5.9$ nm with a very small geometric standard deviation of $\sigma_g = 1.08$. This is in very good agreement with the diameter selected by the deflection conditions.

The success of this new method for depositing size-selected nanoparticles on a silicon substrate for further processing is shown in Fig. 3(b). It can be seen from the SEM micrograph that the particles on the surface are spherical, monodisperse, and non-agglomerated. Neither fragmentation nor deformation of the indium spheres has been observed. It is possible to choose a specific deposition area by the size of the aperture, and the deposition rate can be calculated online from the current measured with the Faraday cup.

In summary, the formation, size-selection, and deposition of indium nanoparticles has been demonstrated. The particles were synthesized in a microwave flow reactor and extracted from the reaction zone by molecular beam sampling.

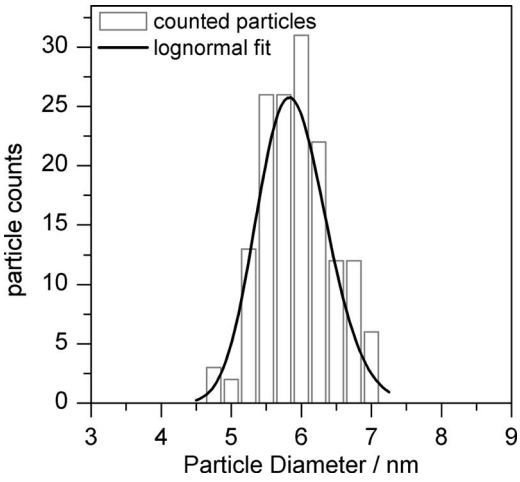

FIG. 4. Image analysis of particles deposited on a TEM-grid. The columns indicate the counted particles, whereas the line indicates the lognormal fit of the data with CMD $= 5.9$ nm and $\sigma_g = 1.08$.

A PMS was used to deflect particles from the molecular beam for size-selected deposition on various surfaces. The particle size was chosen by adjusting the voltage of the deflection capacitor. The preset particle diameter was in excellent agreement with the value obtained from TEM analysis and can be varied by adjusting the deflection voltage. The geometric standard deviation of the size-selected particles was always smaller than 1.1. The particles were spherical, monodisperse, and non-agglomerated. The method described in this work is not limited to certain material combinations and allows the deposition of any gas-supported nanoparticles on almost all solid surfaces. Due to the operating pressure of 10^{-5} mbar and less, this method enables the combination of epitaxial growth processes with nanoparticles deposition techniques in one step and makes a rich variety of material combinations accessible.

Financial support of the German Science Foundation within the Sonderforschungsbereich 445 is gratefully acknowledged. The authors would like to thank Natascha Schlösser and Tim Hülser for their help with microscopy.

[1] D. Beydoun, R. Amal, G. Low, and S. Mcevoy, J. Nanopart. Res. **1**, 439 (1999).
[2] S. Namilae, N. Chandra, and C. Shet, Chem. Phys. Lett. **387**, 247 (2004).
[3] I. Roy, T. Y. Ohulchanskyy, H. E. Pudavar, E. J. Bergey, A. R. Oseroff, J. Morgan, T. J. Dougherty, and P. N. Prasad, J. Am. Chem. Soc. **125**, 7860 (2003).
[4] H.-J. Kim, K. Sung, K.-S. An, Y. K. Lee, C. G. Kim, Y.-H. Lee, and Y. Kim, J. Mater. Chem. **14**, 3396 (2004).
[5] G. M. Credo, M. D. Mason, and S. K. Buratto, Appl. Phys. Lett. **74**, 1978 (1999).
[6] H.-S. Chen, J.-J. Chiu, and T.-P. Perng, Mater. Phys. Mech. **4**, 62 (2001).
[7] H. Ahmed, J. Vac. Sci. Technol. B **15**, 2101 (1997).
[8] W. Seifert, N. Carlsson, M. Miller, M.-EL. Samuelson, and R. Wallenberg, Prog. Cryst. Growth Charact. Mater. **33**, 423 (1996).
[9] D. Bimberg and M. Grundmann, Thin Solid Films **367**, 235 (2000).
[10] S. Paul, C. Pearson, A. Molloy, M. A. Cousins, M. Green, S. Kolliopoulou, P. Dimitrakis, P. Normand, D. Tsoukalas, and M. C. Petty, Nano Lett. **3**, 533 (2003).
[11] C. Binns, Surf. Sci. Rep. **44**, 1 (2001).
[12] F. E. Kruis, H. Fissan, and A. Peled, J. Aerosol Sci. **29**, 511 (1998).
[13] T. Orii, M. Hirasawa, and T. Seto, Appl. Phys. Lett. **83**, 3395 (2003).
[14] H. Kleinwechter, C. Janzen, J. Knipping, H. Wiggers, and P. Roth, J. Mater. Sci. **37**, 4349 (2002).
[15] C. Janzen, H. Kleinwechter, J. Knipping, H. Wiggers, and P. Roth, J. Aerosol Sci. **33**, 833 (2002).
[16] P. Roth and A. Hospital, J. Aerosol Sci. **25**, 61 (1994).
[17] N. Fuchs, Geofis. Pura Appl. **56**, 185 (1963).